ORIGINAL PAPER

A B3LYP and MP2(full) theoretical investigation into the strength of the C–NO$_2$ bond upon the formation of the intermolecular hydrogen-bonding interaction between HF and the nitro group of nitrotriazole or its methyl derivatives

Bao-Hui Li · Wen-jing Shi · Fu-de Ren · Yong Wang

Abstract The changes of bond dissociation energy (*BDE*) in the C–NO$_2$ bond and nitro group charge upon the formation of the intermolecular hydrogen-bonding interaction between HF and the nitro group of 14 kinds of nitrotriazoles or methyl derivatives were investigated using the B3LYP and MP2(full) methods with the 6-311 ++G**, 6-311++G(2df,2p) and aug-cc-pVTZ basis sets. The strength of the C–NO$_2$ bond was enhanced and the charge of nitro group turned more negative in complex in comparison with those in isolated nitrotriazole molecule. The increment of the C–NO$_2$ bond dissociation energies correlated well with the intermolecular H-bonding interaction energies. Electron density shifts analyses showed that the electron density shifted toward the C–NO$_2$ bond upon complex formation, leading to the strengthened C–NO$_2$ bond and the possibly reduced explosive sensitivity.

Keywords Bond dissociation energy in C–NO$_2$ bond · MP2 (full) · Intermolecular hydrogen bond

B.-H. Li
School of Chemistry and Chemical Engineering, Linyi University, Linyi 276005, China

W.-j. Shi (✉)
The Third Hospital of Shanxi Medical University, Taiyuan 030053, China
e-mail: wenjingfd@126.com

F.-d. Ren (✉) · Y. Wang
College of Chemical Engineering and Environment, North University of China, Taiyuan 030051, China
e-mail: fdren888@126.com

Introduction

The search for new and thermally stable insensitive explosive has been a primary goal in the field of energetic material chemistry in order to avoid the catastrophic explosion in use and meet the requirement of military application [1–4]. Therefore, recently much attention has been paid to the investigation on the relationship between the sensitivity and the structure of the energetic compounds [5–17].

For nitro explosives, the X–NO$_2$ (X = C, N or O) bond is relatively weak, and the homolysis of the X–NO$_2$ bond might easily occur in the case of shock or impact. Thus, in most cases, the X–NO$_2$ bond could be termed as "trigger bond" [3, 5, 7, 18]. The energetic compounds with the C–NO$_2$ trigger bond are of vital importance. For a long time, the relationship between the strength of the C–NO$_2$ bond and the explosive sensitivity has been investigated theoretically and experimentally [19, 20]. Li, Xiao and Owens found that, the stronger the C–NO$_2$ bond, the lower the explosive sensitivity became [9, 19, 21]. Furthermore, it has been shown from many theoretical results that, in some cases, the explosive sensitivity of nitro explosive exhibits a good linear relationship with the bond dissociation energy (*BDE*) in the C–NO$_2$ trigger bond [10, 12–14, 17, 18]. For example, the linear correlation between the impact sensitivity $h_{50\%}$ and the ratio (*BDE/E*) of the weakest C–NO$_2$ bond dissociation energy to the total energy *E* was found for the nitroaromatic explosives, including the nitrotriazole energetic compounds [8, 14].

On the other hand, the intermolecular hydrogen bond plays an important role in reducing the explosive sensitivity of the explosives with the potential C–NO$_2$ trigger bond [22]. Sensitivity tests indicated that 1,1-Diamino-2,2-

dinitroethene and [Cu(ethylenediamine)$_2$(nitroformate)$_2$] were insensitive due to the intermolecular H-bond formation [23, 24]. By DFT/BLYP/DNP theoretical method, Tan et al. proposed that the intermolecular hydrogen-bonds among the –NH$_2$ and the –NO$_2$ groups could stabilize nitro compounds [17].

For the explosives with the potential C–NO$_2$ trigger bond, since intermolecular H-bonding interaction influences the explosive sensitivity and the explosive sensitivity shows a linear relationship with the *BDE* in the C–NO$_2$ bond, the intermolecular hydrogen bond might also influence the strength of the C–NO$_2$ bond. Indeed, it is first reported in our recent investigation on the change of the *BDE* in the C–NO$_2$ trigger bond upon the formation of the intermolecular H-bonding interaction between HF and the nitro group of CH$_3$NO$_2$ using the B3LYP and MP2(full) methods. The *BDE* was increased in complex in comparison with that in CH$_3$NO$_2$. Furthermore, the increment of the *BDE* correlated well with the intermolecular hydrogen-bonding interaction energy [25].

As a follow-up to our investigation into the influence of intermolecular H-bonding interaction on the strength of the C–NO$_2$ trigger bond [25], in this paper, we investigated systematically the change of the strength of C–NO$_2$ bond upon the formation of the intermolecular H-bonding interaction between HF and the nitro group of nitrotriazole or its methyl derivatives.

Compounds containing triazole ring can be used as potential outstanding explosives because the heterocyclic ring system confers a high density, thermal stability, high nitrogen content, high volume of detonation products and insensitivity to impact [26–28]. Recently most of the insensitive energetic nitrotriazole explosives with the structural unit 1,2,3-triazole or 1,2,4-triazole have been synthesized [29–33]. Furthermore, it has been shown from many experimental and theoretical results that, for the nitrotriazole explosives, in most cases, a key initiating step appears to be the rupture of the C–NO$_2$ bond [8, 20, 34–40]. The thermal decomposition mechanism proposed is that the nitryl group broke first or left accompanied by the ligand water dissociated from hydrazine 3-nitro-1,2,4-triazol-5-one, (CH$_3$)$_2$NH$_2$C$_2$N$_4$O$_3$H, and Co(H$_2$O)$_6$] (NTO)$_2$·2H$_2$O by means of several experimental methods [34–36]. In theoretical investigations, the scission of C–NO$_2$ was found to be the initial step of the decomposition of NTO at MP2/6-31G** level [37]. The C−NO$_2$ homolysis was confirmed to be the dominant channel for NTO at high temperature by the *ab initio* molecular dynamics method [38]. Li stated that 3-nitro-1,2,4-triazole-5-one and 4-methyl-3,5-dinitro-1,2,4-triazole ignited through the C−NO$_2$ dissociation mechanism [20]. Moreover, population analysis also showed that the C−NO$_2$ bond was the weakest bond in some nitrotriazole compounds [35]. Very recently, the C–NO$_2$ bond has been regarded as the trigger linkage in some nitrotriazoles [39]. These results suggest that the C–NO$_2$ bond might be broken preferentially when nitrotriazole are decomposed, and the C–NO$_2$ bond dissociation energy in nitrotriazoles is possibly one of the important factors affecting the sensitivity.

The investigations into the effect of intermolecular hydrogen bond on the molecular structures of nitrotriazoles have been of great chemical interest in many experimental studies and theoretical calculations. In 1994, Fabio et al. found that the N–H···N hydrogen bond formation caused an obvious change in the length of two N–C bonds for 1,2,4-triazole at HF/6-31G* level [41]. In 2008, the intermolecular H-bonding interaction between 3-nitro-1,2,4-triazol-5-one and HF was studied with density functional theory (DFT) method [42]. In 2009, four complexes constructed by 1,2,3-triazole-4-carboxylate and bipyridyl-like ligands were prepared. It was found that the crystal-lattice water molecules in complexes were connected via intermolecular O–H···O hydrogen bonds into 1D tapes and 2D layers [43]. However, to our knowledge, few theoretical investigations into the influence of the intermolecular H-bonding interaction on the strength of the C–NO$_2$ bond in nitrotriazoles were presented. This theoretical investigation on the change of the strength of C–NO$_2$ bond upon the formation of the HF complex with nitrotriazoles might reveal, in a way, the nature of the change of sensitivity. It will be important for keeping, transporting, safe using, molecular design and synthesis of the important energetic nitrotriazole and its methyl derivatives.

Computational details

The density functional theory (DFT) has emerged as an effective theoretical method to optimize the geometry of energetic compounds. However, to investigate complexation energy, the MP2(full) method with high quality basis set is more reliable [44–46]. Thus, we used the DFT-B3LYP and MP2(full) methods with the 6-311++G**, 6-311++G (2df,2p) and aug-cc-pVTZ basis sets in this work.

All calculations were performed with Gaussian 03 programs [47]. All the nitrotriazole complexes with HF were fully optimized using the DFT-B3LYP and MP2(full) methods with the 6-311++G** and 6-311++G(2df,2p) basis sets. The structures corresponding to the minimum energy points at the molecular energy hypersurface (NImag=0) were obtained. Single point energy calculations were carried out at the B3LYP/6-311++G**, B3LYP/6-311++G(2df,2p), MP2(full)/6-311++G**, MP2(full)/6-311++G(2df,2p) and MP2(full)/aug-cc-pVTZ levels. The shifts of the electron densities [48] that accompanied the formation of complex were displayed at MP2(full)/6-311++G** level.

The *BDE*s of the C–NO$_2$ bond were calculated at the B3LYP/6-311++G**, B3LYP/6-311++G(2df,2p), MP2

(full)/6-311++G**, MP2(full)/6-311++G(2df,2p) and MP2 (full)/aug-cc-pVTZ levels. It is defined as:

$$BDE = E_{(R\cdot)} + E_{(\cdot NO_2)} - E_{(RNO_2)} \quad \text{for nitrotriazole molecule}$$
(1)

$$BDE = E_{(R\cdot)} + E_{(\cdot NO_2 \cdots HF)} - E_{(RNO_2 \cdots HF)} \quad \text{for complex .}$$
(2)

R· means the radical of triazole or its methyl derivative. The *BDE*s were corrected with the basis set superposition error (BSSE) [49, 50] correction.

The intermolecular hydrogen-bonding interaction ($E_{int.}$) was investigated with the definition of the energy difference between the complex and the isolated monomers.

$$E_{int.} = E_{(RNO_2 \cdots HF)} - E_{(RNO_2)} - E_{(HF)}$$
(3)

$E_{int.}$ was also corrected with the BSSE and zero-point energy (ZPE) corrections.

The nitro group charge (Q_{NO2}) was calculated as Eq. 4.

$$Q_{NO_2} = Q_N + Q_{O1} + Q_{O2}$$
(4)

The Q_N, Q_{O1} and Q_{O2} are the charge on the N and O atoms, respectively.

Results and discussion

In this work, the studied HF complexes of nitrotriazole with the structural unit 1,2,3-triazole were 4-nitro-1*H*-1,2,3-triazole···HF (I–1), 4-nitro-3*H*-1,2,3-triazole···HF (I–2), 1-methyl-4-nitro-1,2,3-triazole···HF (I–3), 3-methyl-4-nitro-1,2,3-triazole···HF (I–4), 5-methyl-4-nitro-1*H*-1,2,3-triazole···HF (I–5), 5-methyl-4-nitro-3*H*-1,2,3-triazole···HF (I–6) and 2-methyl-4-nitro-1,2,3-triazole-3-oxide···HF (I–7). Those with the structural unit 1,2,4-triazole were 3-nitro-1*H*-1,2,4-triazole···HF (II–1), 3-nitro-2*H*-1,2,4-triazole···HF (II–2), 1-methyl-3-nitro-1,2,4-triazole···HF (II–3), 2-methyl-3-nitro-1,2,4-triazole···HF (II–4), 5-methyl-3-nitro-1*H*-1,2,4-triazole···HF (II–5), 5-methyl-3-nitro-2*H*-1,2,4-triazole···HF (II–6) and 3-nitro-1*H*-1,2,4-triazole-5-oxide···HF (II–7). The structures of complexes are shown in Fig. 1. The selected geometric parameters are listed in Table 1. The intermolecular hydrogen-bonding interaction energies and the bond dissociation energies in the C–NO$_2$ bond are presented in Tables 2 and 3, respectively. The nitro group charges are collected in Table 4.

Structure of the complex

As can be seen from Fig. 1, all the complexes are C_1 symmetry. All the five membered triazole rings have the planar geometry and the interatomic distances within the triazole ring are not equal. From Table 1, the O3···H5 distances are in the range between 1.827 and 1.883 Å at MP2(full)/6-311++G** level, which fall into the common accepted O···H hydrogen-bond distance. Furthermore, the bond lengths of H7–F10 and N2–O3 bonds increase in complex in comparison with those in the isolated nitrotriazole molecules. These results suggest the formation of the intermolecular hydrogen-bonding interaction between HF and nitro group.

From Table 1, the order of the O3···H5 distance is (I–2) > (I–1) > (I–3) > (I–6) > (I–7) > (I–5) > (I–4) and (II–7) > (II–6) > (II–2) > (II–1) > (II–5) > (II–3) > (II–4) at MP2(full)/6-311++G** level, suggesting that the strength of the intermolecular H-bonding interaction might be I–2 < I–1 < I–3 < I–6 < I–7 < I–5 < I–4 and II–7 < II–6 < II–2 < II–1 < II–5 < II–3 < II–4.

Interestingly, as is shown in Table 1, the bond length of the C–NO$_2$ bond decreases in complexes in comparison with that in isolated nitrotriazole molecules at three levels of theory. It is similar to the change of the C–NO$_2$ trigger-bond length upon the formation of the intermolecular H-bonding interaction between the nitro group of CH$_3$NO$_2$ and HF [25]. In most cases, shortening of a bond length might lead to strengthening of the bond [51]. Thus, the C–NO$_2$ bond might turn stronger upon the formation of the intermolecular hydrogen-bonding interaction.
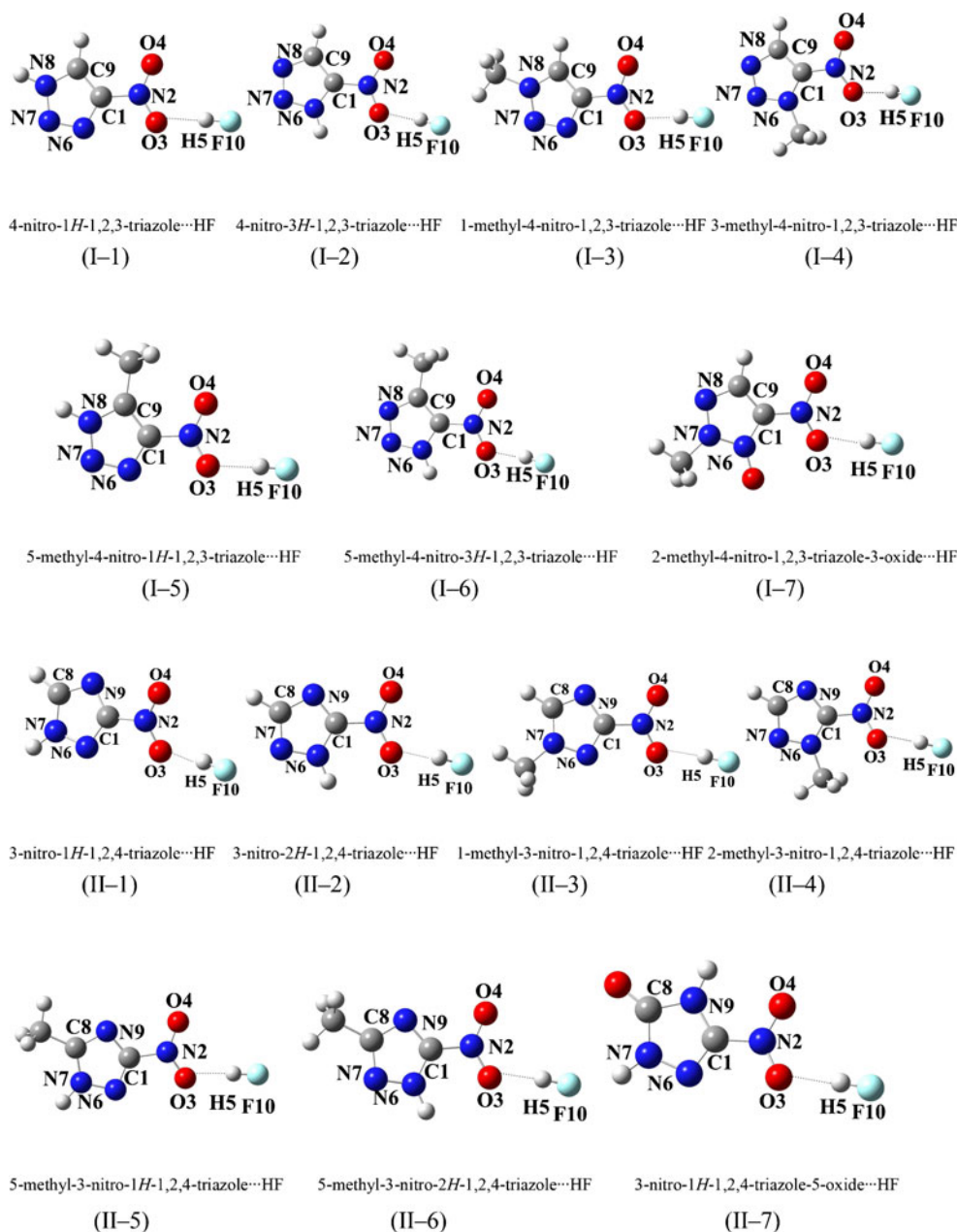
Hydrogen-bonding interaction energies and *BDE* of the C–NO$_2$ bond

From Table 2, the values of the intermolecular hydrogen-bonding interaction energies calculated using the B3LYP method are larger than those obtained from the MP2(full) method. At MP2(full)/aug-cc-pVTZ level, the intermolecular H-bonding interaction energies in the complexes with 1,2,3-triazole unit are within the range of 19.6–26.1 kJmol^{-1} at MP2(full)/aug-cc-pVTZ level (see Table 2). The H-bonding energies in the complexes with 1,2,4-triazole unit are slightly stronger than those in the systems with 1,2,3-triazole unit, and they are up to the range of 20.6–27.7 kJmol^{-1}. At three MP2(full) levels, the H-bonding interaction energies decrease in the same order of I–3 > I–5 > I–7 ≈ I–1 > I–4 > I–6 > I–2 and II–5 > II–3 > II–1 > II–4 > II–6 > II–7 ≈ II–2.

Table 3 gives both uncorrected and corrected *BDE*s of the C–NO$_2$ bond after correction of the BSSE by means of the counterpoise method. At five levels of theory, the proportions of corrected *BDE*s for the complexes to their total *BDE*s, defined as [*BDE*–*BDE*$_{(BSSE)}$]/*BDE*, are all no more than 9.0 %, indicating that the BSSE corrections for *BDE*s are not notable. In general, the BSSE corrections are not negligible. Only in the case of complete basis set, is the correction for BSSE not needed.

From Table 3, for the *BDE* in the C–NO$_2$ bond, the values calculated using the B3LYP method are all lower

4-nitro-1*H*-1,2,3-triazole···HF   4-nitro-3*H*-1,2,3-triazole···HF   1-methyl-4-nitro-1,2,3-triazole···HF   3-methyl-4-nitro-1,2,3-triazole···HF

(I–1)   (I–2)   (I–3)   (I–4)

5-methyl-4-nitro-1*H*-1,2,3-triazole···HF   5-methyl-4-nitro-3*H*-1,2,3-triazole···HF   2-methyl-4-nitro-1,2,3-triazole-3-oxide···HF

(I–5)   (I–6)   (I–7)

3-nitro-1*H*-1,2,4-triazole···HF   3-nitro-2*H*-1,2,4-triazole···HF   1-methyl-3-nitro-1,2,4-triazole···HF   2-methyl-3-nitro-1,2,4-triazole···HF

(II–1)   (II–2)   (II–3)   (II–4)

5-methyl-3-nitro-1*H*-1,2,4-triazole···HF   5-methyl-3-nitro-2*H*-1,2,4-triazole···HF   3-nitro-1*H*-1,2,4-triazole-5-oxide···HF

(II–5)   (II–6)   (II–7)

than those obtained by the MP2(full) method, which is in accordance with our recent investigation [25]. This might be due to that dispersion interaction is not accounted for using the B3LYP method but given by the MP2 method. Thus, the MP2(full) method is more feasible to elucidate the trends in the calculated *BDE*s than the B3LYP method. However, many theoretical investigations have shown that the B3LYP method correctly describes the *BDE* values, and the MP2 method, due to the serious spin contamination, cannot be used to adequately describe *BDE*s [52–55]. In the title compounds, the notable spin contamination was also found for the MP2 method: the value of $<S^2>$ was up to 1.1

for triazole radicals. For the B3LYP method, however, it was about 0.75, and the spin contamination is negligible. Therefore, the B3LYP/6-311++G(2df,2p) method was selected to elucidate the trends in the calculated *BDE*s in this work.

As can be seen from Table 3, at B3LYP/6-311++G (2df,2p) level, the order of the *BDE*s is I–6 > I–5 > I–3 > I–4 > I–7 > I–2 > I–1 or II–3 > II–5 > II–4 > II–1 > II–2 > II–6 > II–7. The *BDE*s in the complexes with nitrotriazole are slightly weaker than those in the systems with the methyl derivative. Furthermore, the *BDE*s in the 1,2,3-triazole complexes are slightly stronger than those in the 1,2,4-triazole systems.

Table 1 Selected geometric parameters (in Å)

Parameters	(I–1)	(I–2)	(I–3)	(I–4)	(I–5)	(I–6)	(I–7)
O3···H5	1.818[a]	1.822	1.807	1.805	1.800	1.806	1.809
	1.814[b]	1.825	1.805	1.810	1.799	1.810	1.808
	1.856[c]	1.860	1.854	1.837	1.846	1.849	1.847
C1–N2	1.442[a] (1.450)	1.427 (1.435)	1.440 (1.448)	1.427 (1.436)	1.435 (1.444)	1.419 (1.428)	1.420 (1.430)
	1.438[b] (1.445)	1.423 (1.430)	1.436 (1.443)	1.423 (1.431)	1.430 (1.439)	1.415 (1.424)	1.416 (1.426)
	1.447[c] (1.452)	1.432 (1.438)	1.446 (1.451)	1.432 (1.438)	1.442 (1.448)	1.428 (1.434)	1.423 (1.431)
N2–O3	1.228 (1.217)	1.241 (1.221)	1.229 (1.217)	1.241 (1.223)	1.229 (1.217)	1.243 (1.224)	1.233 (1.221)
	1.226 (1.215)	1.239 (1.219)	1.227 (1.215)	1.239 (1.221)	1.227 (1.215)	1.241 (1.222)	1.231 (1.219)
	1.230 (1.225)	1.239 (1.228)	1.231 (1.226)	1.239 (1.229)	1.231 (1.225)	1.240 (1.230)	1.236 (1.230)
H5–F10[d]	0.935	0.934	0.935	0.935	0.936	0.935	0.935
	0.935	0.933	0.935	0.934	0.936	0.934	0.935
	0.925	0.924	0.926	0.925	0.926	0.925	0.926
Parameters	(II–1)	(II–2)	(II–3)	(II–4)	(II–5)	(II–6)	(II–7)
O3···H5	1.802	1.816	1.792	1.799	1.791	1.808	1.839
	1.801	1.822	1.792	1.803	1.791	1.814	1.838
	1.840	1.850	1.830	1.827	1.836	1.858	1.883
C1–N2	1.463 (1.470)	1.448 (1.456)	1.461 (1.469)	1.448 (1.457)	1.462 (1.469)	1.448 (1.456)	1.442 (1.451)
	1.459 (1.466)	1.445 (1.451)	1.457 (1.464)	1.445 (1.452)	1.458 (1.464)	1.444 (1.451)	1.438 (1.446)
	1.453 (1.460)	1.442 (1.448)	1.452 (1.459)	1.441 (1.448)	1.454 (1.459)	1.441 (1.446)	1.440 (1.446)
N2–O3	1.231 (1.219)	1.242 (1.212)	1.232 (1.219)	1.242 (1.214)	1.232 (1.220)	1.242 (1.213)	1.226 (1.215)
	1.229 (1.217)	1.239 (1.211)	1.230 (1.217)	1.240 (1.212)	1.230 (1.217)	1.240 (1.211)	1.224 (1.213)
	1.234 (1.228)	1.240 (1.225)	1.235 (1.229)	1.241 (1.226)	1.234 (1.229)	1.241 (1.226)	1.230 (1.225)
H5–F10	0.936	0.934	0.936	0.935	0.936	0.934	0.934
	0.935	0.933	0.936	0.935	0.936	0.934	0.933
	0.926	0.925	0.927	0.926	0.927	0.925	0.924

The values in parenthesis are the geometric parameters for isolated nitrotriazole molecules

[a] At B3LYP/6-311++G** level

[b] At B3LYP/6-311++G(2df,2p) level

[c] At MP2(full)/6-311++G** level

[d] The H–F bond length in HF is 0.922, 0.922 and 0.916 Å at B3LYP/6-311++G**, B3LYP/6-311++G(2df,2p) and MP2(full)/6-311++G** levels, respectively

Interestingly, from Table 3, the *BDE*s in the C–NO$_2$ bond in complexes are larger than those in the corresponding isolated nitrotriazole molecules. This result suggests that the strength of the C–NO$_2$ bond is enhanced upon the formation of intermolecular H-bonding interaction between HF and the nitro group, which is in agreement with the analysis of structure. In the investigation on the CH$_3$NO$_2$ complex with HF, we have also found that the strength of the C–NO$_2$ trigger bond is enhanced [25]. The stronger the C–NO$_2$ trigger bond in nitro explosives, in most cases, the lower the explosive sensitivity turned [18, 22, 23]. Thus, it is possible that the explosive sensitivity of nitrotriazoles is reduced upon the formation of intermolecular H-bonding interaction. It should be noted that it has not been established if the C–NO$_2$ bonds are the

trigger linkages in all the title compounds. In fact, breaking of the C–NO$_2$ bond is not the only mechanism for initiating detonation. There might be many others for nitrotriazole molecules, such as formation of nitrosoaromatic intermediates, reactions of the –NO$_2$ group with an *ortho* substituent, etc. [38, 56–58]. Moreover, many factors are involved in sensitivity. Therefore, the strengthened C–NO$_2$ bond does not in all cases lead to the reduced sensitivity for nitrotriazoles.

As can be seen from Tables 2 and 3, the value of the increment of the *BDE* in complex in comparison with that of the corresponding isolated nitrotriazole molecule (Δ*BDE*) is very close to the intermolecular hydrogen-bonding interaction energy. For instance, for the hydrogen-bonded complexes with 1,2,3-triazole, the Δ*BDE*s are in the range of 20.3–26.8 kJmol^{-1} at B3LYP/6-311++G(2df,2p) level. This

Table 2 Intermolecular hydrogen-bonding interaction energy ($-E_{int.}$(kJmol^{-1}))

Parameters	(I–1)	(I–2)	(I–3)	(I–4)	(I–5)	(I–6)	(I–7)
B3LYP/6-311++G**	27.4 (25.0)	24.1 (22.1)	28.9 (26.4)	25.9 (23.2)	27.0 (20.5)	26.0 (23.5)	25.9 (19.7)
	18.5	*16.1*	*19.9*	*16.7*	*19.7*	*20.5*	*19.7*
B3LYP/6-311++G(2df,2p)	28.8 (29.3)	22.5 (20.5)	28.0 (26.1)	24.7 (22.5)	28.7 (26.8)	24.8 (22.8)	28.2 (26.2)
	22.1	*13.8*	*18.9*	*15.6*	*19.6*	*15.8*	*19.2*
MP2(full)/6-311++G**	21.9 (16.2)	16.9 (9.6)	23.1 (17.3)	18.9 (10.8)	22.8 (15.8)	18.3 (10.9)	22.1 (14.8)
MP2(full)/6-311++G(2df,2p)	23.3 (18.1)	17.7 (12.3)	24.6 (19.3)	20.3 (14.5)	24.4 (18.9)	19.7 (14.0)	23.3 (17.5)
MP2(full)/aug-cc-pVTZ	24.3 (18.4)	19.6 (14.4)	26.1 (20.5)	21.9 (16.1)	26.0 (20.6)	21.3 (16.0)	25.0 (19.5)
Parameters	(II–1)	(II–2)	(II–3)	(II–4)	(II–5)	(II–6)	(II–7)
B3LYP/6-311++G**	28.9 (26.3)	24.0 (21.3)	30.3 (27.7)	26.5 (23.7)	30.4 (27.8)	25.7 (23.1)	23.2 (20.7)
	19.2	*15.1*	*20.7*	*17.2*	*20.8*	*16.9*	*14.5*
B3LYP/6-311++G(2df,2p)	29.3 (27.2)	26.1 (27.4)	31.6 (29.7)	25.2 (23.0)	29.4 (27.4)	24.0 (21.9)	20.8 (18.9)
	19.8	*20.6*	*22.4*	*15.9*	*20.0*	*15.0*	*12.2*
MP2(full)/6-311++G**	23.2 (16.0)	18.0 (10.3)	24.5 (17.2)	20.5 (12.0)	24.9 (18.7)	20.0 (14.0)	17.9 (11.9)
MP2(full)/6-311++G(2df,2p)	24.5 (18.9)	18.8 (13.1)	25.5 (19.9)	21.3 (15.2)	25.8 (20.5)	20.7 (15.3)	18.8 (13.8)
MP2(full)/aug-cc-pVTZ	26.0 (20.5)	20.7 (15.4)	27.5 (21.8)	23.3 (17.5)	27.7 (22.0)	22.5 (17.0)	20.6 (15.2)

The values in the parenthesis are BSSE-corrected ($-E_{int.(BSSE)}$), and those with BSSE and ZPE ($-E_{int.(BSSE-ZPE)}$) correction are in italic

is pleasing information: the explosive complex needs not only more energy to destroy the intermolecular hydrogen-bonding interaction, but also to counteract the increment of the *BDE* in the C–NO$_2$ bond in the process of detonation. Therefore, if the C–NO$_2$ bonds are the trigger linkages, the origin of the change of explosive sensitivity is not only due

Table 3 Bond dissociation energy (*BDE* (kJmol^{-1})) in the C–NO$_2$ bond

Parameters	(I–1)	(I–2)	(I–3)	(I–4)	(I–5)	(I–6)	(I–7)
B3LYP/6-311++G**	330.0 (321.6)	328.6 (320.9)	334.9 (326.5)	330.6 (321.8)	342.4 (333.6)	340.5 (332.1)	331.6 (323.1)
	306.7 (298.9)	*308.6 (301.5)*	*309.8 (302.1)*	*307.6 (299.9)*	*316.3 (308.2)*	*317.6 (309.9)*	*306.5 (298.8)*
B3LYP/6-311++G(2df,2p)	335.2 (329.8)	337.6 (335.5)	339.9 (334.4)	339.2 (336.8)	347.8 (342.0)	348.9 (345.9)	337.7 (331.9)
	313.6 (309.5)	*316.3 (312.5)*	*316.3 (312.2)*	*315.7 (312.5)*	*322.4 (317.1)*	*324.3 (319.2)*	*314.0 (310.9)*
MP2(full)/6-311++G**	419.6 (382.7)	425.6 (393.3)	423.4 (391.3)	424.4 (389.1)	434.0 (398.7)	440.0 (401.3)	465.7 (427.1)
	385.0 (376.4)	*392.6 (380.1)*	*385.3 (379.0)*	*423.7 (391.6)*	*395.6 (388.7)*	*416.8 (387.4)*	*426.9 (389.3)*
MP2(full)/6-311++G(2df,2p)	456.6 (436.2)	459.6 (432.0)	453.8 (430.4)	458.0 (432.7)	465.7 (441.1)	482.1 (447.9)	486.4 (452.5)
	434.8 (407.2)	*399.6 (379.4)*	*401.1 (375.5)*	*408.7 (378.3)*	*418.4 (393.4)*	*455.8 (431.9)*	*449.2 (416.5)*
MP2(full)/aug-cc-pVTZ	465.6 (430.9)	464.8 (435.6)	465.3 (433.7)	466.1 (434.7)	472.9 (442.6)	481.7 (454.9)	514.4 (482.1)
	428.9 (411.5)	*465.2 (439.8)*	*423.9 (405.7)*	*433.3 (417.0)*	*436.2 (406.5)*	*479.0 (453.6)*	*465.4 (431.3)*
Parameters	(II–1)	(II–2)	(II–3)	(II–4)	(II–5)	(II–6)	(II–7)
B3LYP/6-311++G**	314.4 (306.2)	310.5 (302.9)	319.4 (311.2)	313.5 (305.1)	319.8 (311.7)	314.2 (306.7)	306.6 (298.8)
	289.8 (282.4)	*290.0 (282.9)*	*294.0 (286.6)*	*289.4 (281.6)*	*293.6 (286.3)*	*291.8 (284.7)*	*287.0 (279.7)*
B3LYP/6-311++G(2df,2p)	321.1 (317.9)	319.8 (319.0)	325.4 (322.2)	323.3 (322.9)	323.7 (318.4)	318.8 (313.4)	311.0 (305.4)
	293.5 (289.2)	*298.7 (296.3)*	*294.4 (290.2)*	*299.0 (297.5)*	*298.6 (294.1)*	*299.2 (295.5)*	*294.7 (290.9)*
MP2(full)/6-311++G**	380.9 (347.7)	378.4 (345.7)	381.3 (347.9)	381.6 (345.3)	385.3 (347.3)	379.4 (347.3)	375.0 (343.1)
	344.8 (313.7)	*347.5 (316.1)*	*342.6 (311.0)*	*346.8 (312.9)*	*345.5 (314.0)*	*345.7 (313.8)*	*343.3 (311.9)*
MP2(full)/6-311++G(2df,2p)	408.3 (385.4)	392.5 (363.3)	393.8 (364.2)	396.8 (365.2)	398.3 (469.1)	393.5 (364.0)	391.1 (362.0)
	358.5 (330.5)	*363.0 (334.8)*	*374.2 (351.4)*	*363.6 (333.3)*	*377.5 (358.1)*	*360.9 (332.4)*	*360.3 (332.0)*
MP2(full)/aug-cc-pVTZ	413.9 (386.4)	413.6 (385.2)	414.4 (386.6)	419.0 (388.3)	418.9 (389.8)	414.5 (385.0)	413.5 (384.0)
	377.6 (352.3)	*384.7 (357.1)*	*390.2 (369.3)*	*386.8 (357.0)*	*380.6 (352.6)*	*382.5 (354.1)*	*378.2 (349.1)*

The values in the parenthesis are BSSE-corrected (–Eint.(BSSE)), and those of the bond dissociation energies for isolated nitrotriazole molecules are in italic

Table 4 Charges (in e) of nitro group

Parameters	(I–1)	(I–2)	(I–3)	(I–4)	(I–5)	(I–6)	(I–7)
Mulliken charge[a]	−0.240 (−0.194)	−0.312 (−0.237)	−0.251 (−0.205)	−0.374 (−0.278)	−0.298 (−0.228)	−0.342 (−0.255)	−0.290 (−0.246)
Natural charge[a]	−0.275 (−0.267)	−0.281 (−0.268)	−0.276 (−0.273)	−0.288 (−0.276)	−0.288 (−0.280)	−0.300 (−0.286)	−0.274 (−0.260)
APT charge[b]	−0.067 (−0.035)	−0.017 (−0.015)	−0.067 (−0.034)	−0.031 (−0.003)	−0.070 (−0.035)	−0.021 (0.015)	−0.003 (0.044)
Parameters	(II–1)	(II–2)	(II–3)	(II–4)	(II–5)	(II–6)	(II–7)
Mulliken charge[a]	−0.287 (−0.227)	−0.303 (−0.241)	−0.314 (−0.251)	−0.359 (−0.272)	−0.289 (−0.269)	−0.322 (−0.286)	−0.270 (−0.230)
Natural charge[a]	−0.256 (0.253)	−0.260 (0.242)	−0.263 (−0.259)	−0.268 (−0.259)	−0.263 (−0.258)	−0.266 (−0.256)	−0.263 (−0.251)
APT charge[b]	−0.097 (−0.060)	−0.044 (−0.013)	−0.096 (−0.060)	−0.049 (−0.016)	−0.103 (−0.064)	−0.045 (−0.013)	−0.023 (0.010)

The values in parenthesis are the charges for isolated nitrotriazole molecules

[a] At MP2(full)/6-311++G** level

[b] At B3LYP/6-311++G(2df,2p) level

to the formation of the intermolecular H-bonding interaction but also due to the increment of the C–NO$_2$ bond dissociation energy. In the previous investigations, the influence of the intermolecular H-bonding interaction on the strength of the C–NO$_2$ bond was not considered, and only the formation of intermolecular H-bonding interaction was regarded as the origin of the change of explosive sensitivity [19].

From Tables 2 and 3, although the order of the H-bonding interaction energies is not in accordance with that of the C–NO$_2$ bond dissociation energy, it is just in agreement with the order of the increment of the C–NO$_2$ bond dissociation energies. The relationship between the H-bonding interaction energy and increment of the C–NO$_2$ bond dissociation energy (ΔBDE) is shown in Fig. 2 at B3LYP/6-311++G(2df,2p) level. The correlation coefficient is 0.9751 or 0.9705 for the
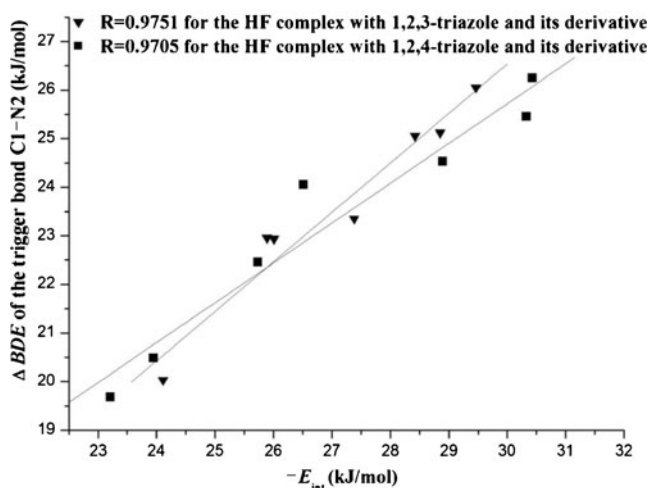
hydrogen-bonded complexes with the 1,2,3-triazole or 1,2,4-triazole unit, respectively. They fit the following equations:

$$\Delta BDE = 1.018(-E_{int.}) - 4.010 \tag{5}$$

$$\Delta BDE = 0.820(-E_{int.}) + 1.132. \tag{6}$$

ΔBDE and $-E_{int.}$ are in kJ·mol^{-1}. This result shows again that the intermolecular H-bonding interaction has an important effect on the strength of the C–NO$_2$ bond.

Charge of nitro group

From Table 4, three kinds of charges (Mulliken, Natural and APT charges) of nitro group in complexes are all more negative than those in the corresponding isolated nitrotriazole molecules. In particular, in 5-methyl-4-nitro-3H-1,2,3-triazole, 2-methyl-4-nitro-1,2,3-triazole-3-oxide and 3-nitro-1H-1,2,4-triazole-5-oxide, the values of the APT charge are positive. However, in their corresponding complexes I–6, I–7 and II–7, they turn negative. These results show that more negative charges concentrate on the nitro group upon the formation of complexes. The more negative charges the nitro groups carry, the lower sensitivities the explosives show [15–17]. Therefore, it is possible that the sensitivity is reduced with the formation of complexes, which is in accordance with the above analysis.

Analysis of the electron density shifts

In order to obtain deeper insight into the origin of the change of the C–NO$_2$ bond strength, the analysis of the electron density shifts which accompanied the H-bonding formation by the initial nitrotriazoles followed by addition of HF was carried out. For this purpose, the electron density shift was

Fig. 2 The increment of the C–NO$_2$ bond dissociation energy (ΔBDE) in complex in comparison with the isolated nitrotriazole molecules versus the intermolecular H-bonding interaction energy ($-E_{int.}$) at B3LYP/6-311++G(2df,2p) level

calculated by evaluating the difference between the total electron densities of complex and individual monomers.

$$\rho_{shift} = \rho_{(RNO_2\cdots HF)} - \rho_{RNO_2} - \rho_{HF}$$

The shifts of electron density were illustrated in Fig. 3. Purple regions represented the accumulation of additional electron density; yellow regions indicated loss of density.

The H-bonding formations are shown by the yellow region around the hydrogen atom of the H–F bond and the purple region surrounding the oxygen atom of the nitro group, consistent with the accepted notion that the hydrogen atom loses density. The loss of the hydrogen atom density weakens the H–F bond, leading to the elongation of the H–F bond, as is in common with the feature of the conventional H-bond.
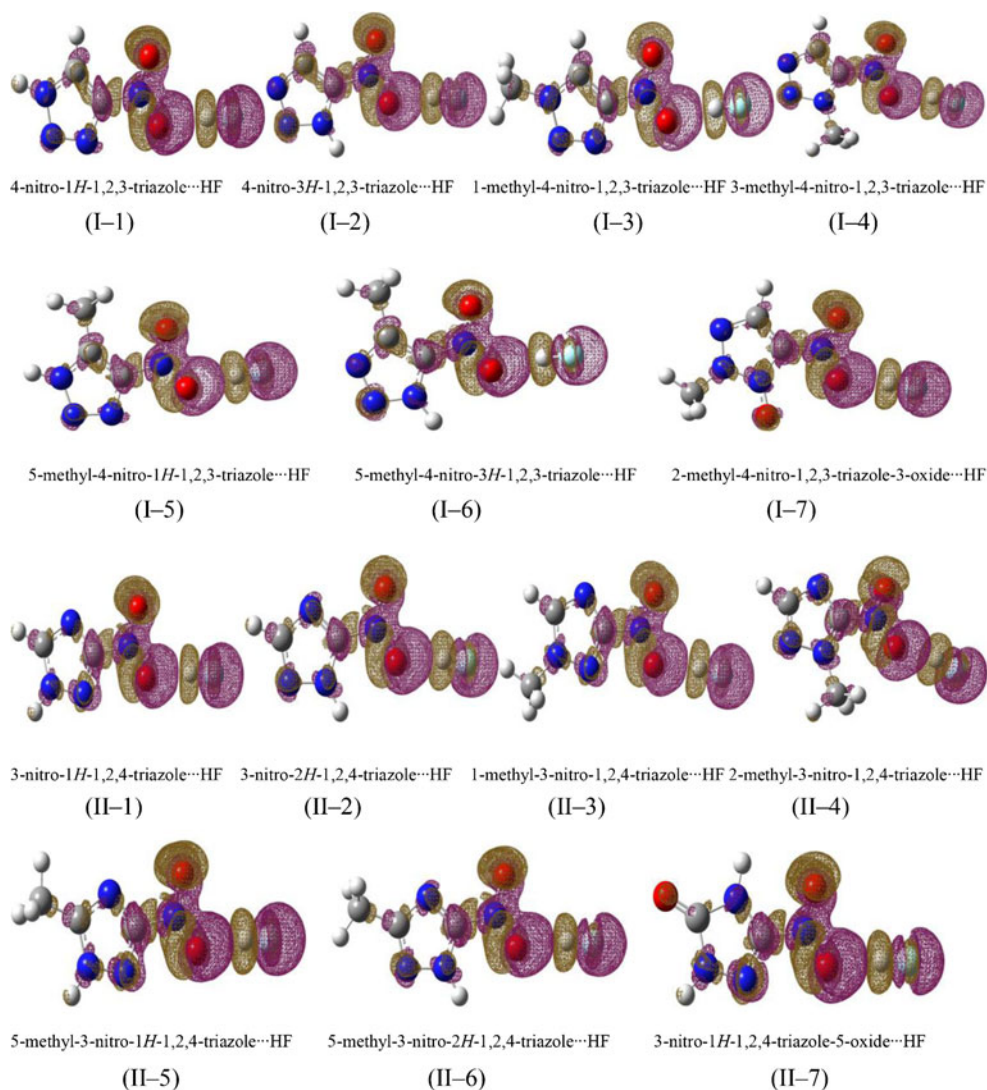
It is interesting that much purple area is around the C and N atoms of the C–NO$_2$ bond and extending toward the C–NO$_2$ bond, showing that the electron density shifts toward the C and N atoms as well as the C–NO$_2$ bond. It is well known that, the more intensive the electron between two atoms, the more chances of overlapping. As a result, the strength of the C–NO$_2$ bond is improved. Thus, we can draw a conclusion that the electron density shifts toward the C–NO$_2$ bond upon the formation of the H-bonding interaction between HF and the nitro group, leading to the enhanced C–NO$_2$ bond and the possibly reduced sensitivity of explosive.

Conclusions

We investigated the changes of the *BDE* in the C–NO$_2$ bond and nitro group charge upon the formation of the intermolecular hydrogen-bonding interaction between HF and the nitro group of 14 kinds of nitrotriazoles or methyl derivatives using the B3LYP and MP2(full) methods. The strength of the C–NO$_2$ bond was enhanced and the charge of nitro group turned more negative upon complexation. The value of Δ*BDE* correlated well with the intermolecular H-bonding

Fig. 3 Shifts of electron density as a result of the formation of complexes

4-nitro-1*H*-1,2,3-triazole···HF 4-nitro-3*H*-1,2,3-triazole···HF 1-methyl-4-nitro-1,2,3-triazole···HF 3-methyl-4-nitro-1,2,3-triazole···HF

(I–1)   (I–2)   (I–3)   (I–4)

5-methyl-4-nitro-1*H*-1,2,3-triazole···HF 5-methyl-4-nitro-3*H*-1,2,3-triazole···HF 2-methyl-4-nitro-1,2,3-triazole-3-oxide···HF

(I–5)   (I–6)   (I–7)

3-nitro-1*H*-1,2,4-triazole···HF 3-nitro-2*H*-1,2,4-triazole···HF 1-methyl-3-nitro-1,2,4-triazole···HF 2-methyl-3-nitro-1,2,4-triazole···HF

(II–1)   (II–2)   (II–3)   (II–4)

5-methyl-3-nitro-1*H*-1,2,4-triazole···HF 5-methyl-3-nitro-2*H*-1,2,4-triazole···HF 3-nitro-1*H*-1,2,4-triazole-5-oxide···HF

(II–5)   (II–6)   (II–7)

interaction energy. The electron density shifted toward the C–NO$_2$ bond upon complex formation, leading to the strengthened C–NO$_2$ bond and the possibly reduced explosive sensitivity.

References

1. Hu TP, Ren FD, Ren J (2009) J Mol Struct (THEOCHEM) 909:13–18
2. Richard RM, Ball DW (2008) J Mol Struct (THEOCHEM) 851:284–293
3. Qiu L, Gong XD, Zheng J, Xiao HM (2009) J Hazard Mater 166:931–938
4. Wang GX, Gong XD, Liu Y, Xiao HM (2009) Spectrochim Acta Part A 74:569–574
5. Liu Y, Gong XD, Wang LJ, Wang GX, Xiao HM (2011) J Phys Chem A 115:1754–1762
6. Keshavarz MH, Pouretedal HR (2010) Propell Explos Pyrot 35:175–181
7. Pospíšil M, Vávra P, Concha MC, Murray JS, Politzer P (2010) J Mol Model 16:895–901
8. Zhao J, Xu DH, Cheng XL (2010) Struct Chem 21:1235–1240
9. Li JS (2010) J Hazard Mater 174:728–733
10. Li JS (2010) J Hazard Mater 180:768–772
11. Atalar T, Jungová M, Zeman S (2009) J Energ Mater 27:200–216
12. Cao CZ, Gao S (2007) J Phys Chem B 111:12399–12402
13. Zhao J, Cheng XL, He B, Yang XD (2006) Struct Chem 17:501–507
14. Song XS, Cheng XL, Yang XD, He B (2006) Propell Explos Pyrot 31:306–310
15. Zhang CY, Shu YJ, Huang YG, Zhao XD, Dong HS (2005) J Phys Chem B 109:8978–8982
16. Rice BM, Hare JJ (2002) J Phys Chem A 106:1770–1783
17. Tan BS, Long XP, Peng RF, Li HB, Jin B, Chu SJ, Dong HS (2010) J Hazard Mater 183:908–912
18. Delpuech A, Cherville J (1979) Propell Explos Pyrot 4:121–128
19. Xiao HM (1994) Molecular orbital theory of nitro-compound. Publishing House of Defense Industry, Peking
20. Li JS (2010) J Phys Chem B 114:2198–2202
21. Owens FJ, Jayasuriya K, Abrahmsen L, Politzer P (1985) Chem Phys Lett 116:434–438
22. Ren WZ, Wang ZS (2004) Explosive theory and practice. China North Chemical Industries Corp Press, Nanjing
23. Yang L, Zhang J, Zhang T, Zhang J, Cui Y (2009) J Hazard Mater 164:962–967
24. Buszewski B, Michel M, Cudziło S, Chyłek Z (2009) J Hazard Mater 164:1051–1058
25. Wang HB, Shi WJ, Ren FD, Yang L, Wang JL (2012) Comp Theor Chem doi:10.1016/j.comptc.2012.06.018
26. Xue H, Gao Y, Wamley BT, Shreeve JM (2005) Chem Mater 17:191–198
27. Sikder AK, Geetha M, Sarwade DB, Agrrawal JP (2001) J Hazard Mater A 82:1–12
28. Li XH, Zhang RZ, Zhang XZ (2011) Struct Chem 22:577–587
29. Vereshchyagin LI, Pokatilov FA, Kizhnyaev VN (2008) Chem Heterocycl Compd 44:3–25
30. Sukhanov GT, Sukhanova AG, Lukin AY (2007) Chem Heterocycl Compd 43:786–792
31. Sukhanova AG, Sakovich GV, Sukhanov GT (2008) Chem Heterocycl Compd 44:1368–1373
32. Duddu R, Dave PR, Damavarapu R, Surapaneni R, Parrish D (2009) Synth Commun 39:4282–4288
33. Darren LN, Michael AH, Herbert HH (2003) J Energ Mater 21:57–62
34. Yi JH, Zhao FQ, Ren YH, Xu SY, Ma HX, Hu RZ (2010) J Therm Anal Calorim 100:623–627
35. Ma HX, Song JR, Hu RZ, Zhai GH, Xu KZ, Wen ZY (2004) J Mol Struct (THEOCHEM) 678:217–222
36. Song JR, Ma HX, Huang J, Hu RZ (2004) Thermochim Acta 416:43–46
37. Wang YM, Chen C, Lin ST (1999) J Mol Struct (THEOCHEM) 460:79–102
38. Yim WL, Liu ZF (2001) J Am Chem Soc 10:2243–2250
39. Ravi P, Babu BK, Tewari SP (2012) J Mol Model. doi:10.1007/s00894-012-1515-z
40. Pourmortazavi SM, Rahimi-Nasrabadi M, Kohsari I, Hajimirsadeghi SS (2011) J Therm Anal Calorim. doi:10.1007/s10973-011-1845-6
41. Fabio R, Luigi B, Gustavo P, Aldo D (1994) Struct Chem 1:1–7
42. Fang G, Xu L, Hu X, Li X (2008) J Hazard Mater 160:51–55
43. Zheng ZB, Wu RT, Li JK, Sun YF (2009) J Mol Struct 928 (2009):78–84
44. Richard RM, Ball DW (2007) J Mol Struct (THEOCHEM) 806:113–120
45. Tanaka N, Tamezane T, Nishikiori H, Fujii T (2003) J Mol Struct (THEOCHEM) 631:21–28
46. Novoa JJ, Mota F (2000) Chem Phys Lett 318:345–354
47. Frisch MJ et al. (2003) Gaussian 03, Revision B.03, Gaussian Inc, Pittsburgh, PA
48. Scheiner S, Kar T (2002) J Phys Chem A 106:1784–1789
49. Duijineveldt FB, Duijineveldt-van de Rijdt JCMV, Lenthe JHV (1994) Chem Rev 94:1873–1885
50. Boys SF, Bernardi F (1970) Mol Phys 19:553–566
51. Macaveiu L, Göbel M, Klapötke TM, Murray JS, Politzer P (2010) Struct Chem 21:139–146
52. Budyka MF, Zyubina TS, Zarkadis AK (2002) J Mol Struct (THEOCHEM) 594:113–125
53. Jursic BS (1996) J Mol Struct (THEOCHEM) 366:103–108
54. Brinck T, Haeberlin M, Jonsson M (1997) J Am Chem Soc 119:4239–4244
55. Barckholtz C, Barckholtz TA, Hadad CM (1999) J Am Chem Soc 121:491–500
56. Brill TB, James KJ (1993) Chem Rev 93:2667–2692
57. Murray JS, Concha MC, Politzer P (2009) Mol Phys 107:89–97
58. Politzer P, Lane P, Murray JS (2011) Cent Europ J Energ Mater 8:39–52